Electronic Supplementary Material (ESI) for Chemical Science.
This journal is © The Royal Society of Chemistry 2023

Electronic Supplementary Information for

Site-specific Chirality-conferred Structural Compaction Differentially Mediates the Cytotoxicity of Aβ42

*Gongyu Li,[*a,c‡] Chae Kyung Jeon,[d‡] Min Ma,[b‡] Yifei Jia,[a] Zhen Zheng,[f] Daniel G. Delafield,[b] Gaoyuan Lu,[b] Elena V. Romanova,[e] Jonathan V. Sweedler,[e] Brandon T. Ruotolo*[d] and Lingjun Li*[b]*

[a]State Key Laboratory of Pharmaceutical Chemical Biology, Research Center for Analytical Science and Tianjin Key Laboratory of Biosensing and Molecular Recognition, Frontiers Science Center for New Organic Matter, College of Chemistry, Nankai University, Tianjin 300071, China.

[b]School of Pharmacy and Department of Chemistry, University of Wisconsin-Madison, 777 Highland Ave., Madison, WI 53705, USA.

[c]Haihe Laboratory of Sustainable Chemical Transformations, Tianjin 300192, China.

[d]Department of Chemistry, University of Michigan, Ann Arbor, MI 48109, USA.

[e]Department of Chemistry and The Beckman Institute for Advanced Science and Technology, University of Illinois at Urbana−Champaign, Urbana, Illinois 61801, USA.

[f]School of Pharmacy, Tianjin Medical University, Tianjin 300070, China.

‡ G.L., C.K.J. and M.M. contributed equally to this work.

Correspondence:
Prof. Dr. Gongyu Li
Email: ligongyu@nankai.edu.cn
Prof. Dr. Brandon T. Ruotolo
Email: bruotolo@umich.edu
Prof. Dr. Lingjun Li
Email: lingjun.li@wisc.edu

Table of Contents:

Supplementary Experimental

D-Aβ Customization. We designed these peptide stereoisomeric pairs with the aim of construction for the model of site-specific, domain-constrained Aβ42 isoforms. It has been reported that simultaneous D-isomerization of Asp7 and Asp23 of Aβ42 could enhance Aβ42 neurotoxicity and fibril formation (*Biochem. Biophys. Res. Commun.* 2013, 441, 493-498). However, it is still not clear if the D-isomerization in real living systems would happen in a region-selective manner or not, which means one can anticipate detecting Aβ42 isoforms with amino acid-selective D-substitutions. To systematically inspect the role of D-isomerization at Asp and Ser, two most frequently observed naturally occurring residues in AD brain, we therefore customized 12 Aβ stereoisomers in three groups to inspect domain-constrained chiral effects (Tables 1/2). Amyloid β peptides with D- and L-forms as designed were supplied by GenScript USA, Inc. (Piscataway, NJ). To keep the enantiopurity during peptide synthesis, it is important to ensure the enantiopurity of raw amino acid materials and to add anti-racemization reagents during condensation. Chemical peptide synthesis procedures were used, the final purities of all Aβ isoforms are higher than 95% with standard RPLC-MS protocol and no further purification was performed for all Aβ isoforms upon arrival.

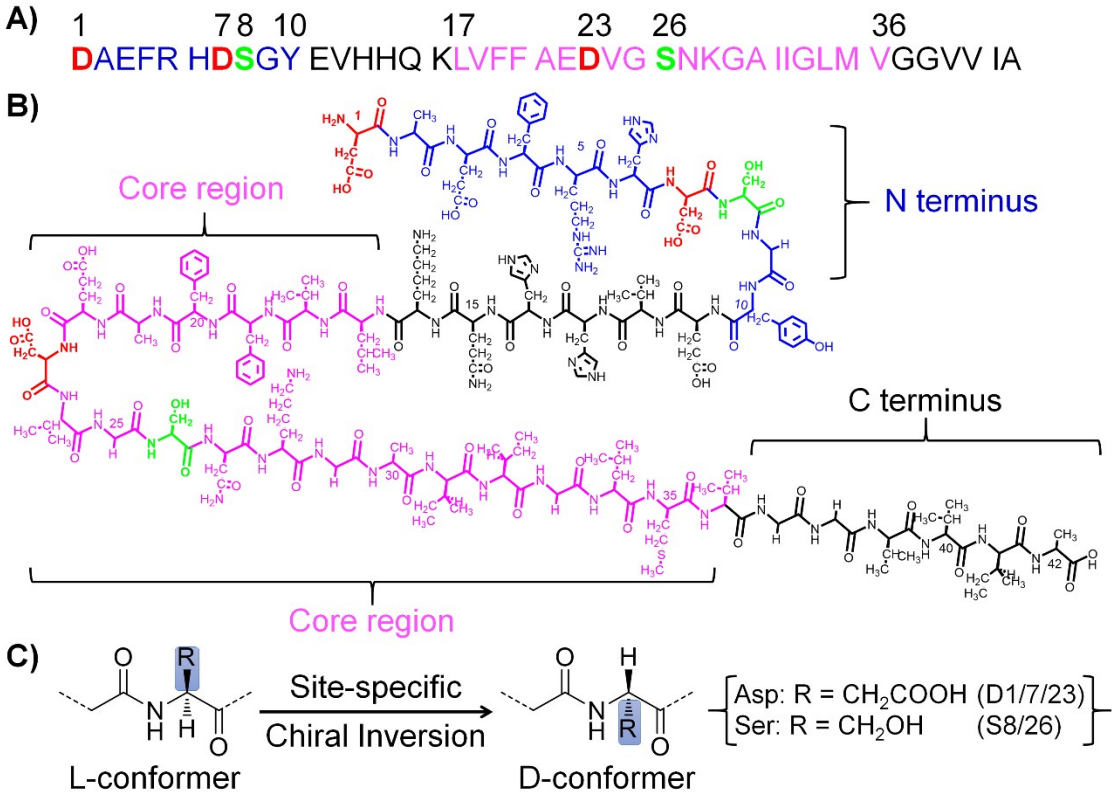

Scheme S1. Structural elements of Aβ and epitope domain-constrained structural flips as induced by site-specific chiral inversion. A) Primary sequence for full-length Aβ42, highlighted with Asp (D)/Ser (S) residues and key functional elements (N terminus and Core region). B) Chemical structure. C) Chiral inversions involved in this study.

Chemicals. Chemicals (including copper acetate salt, ammonium acetate) and protein samples (HSA/BSA) were obtained from Sigma-Aldrich (St. Louis, MO). Thiazolyl Blue Tetrazolium Bromide (MTT, >97.5%) powder suitable for cell culture, hydrochloric acid (36.5-38.0% for molecular biology), and triton X-100 for molecular biology are purchased from BioReagent. No further purification was performed for the

reagents. All solvents used in this study were of HPLC grade supplied by Sigma-Aldrich (St. Louis, MO). Purified water (conductivity of 18.2 MΩ.cm) was obtained from a Milli-Q® Reference System (Millipore Corp., Bedford, MA, USA).

Improved Aβ42 sample preparation for native nESI-MS.

1) Dissolve 5 mg Aβ42 peptide (supplied by Genscript) into 500 μL 1% ammonium hydroxide (or DMSO if unsolvable in $NH_3 \cdot H_2O$) and vortex briefly. (Notably, the peptide quality/purity is key to obtain a good suspension for further experiments.)
2) Lyophilize (freeze dry, -50 ℃ and ~50 mTorr) overnight.
3) Dissolve lyophilized stock in 500 μL of ammonium acetate (10 mM, pH 6.8), and vortex/sonicate briefly. The concentration was determined by UV measurements on a Thermo NanoDrop 2000c instrument (ε coefficient = 1490 for Aβ42).
4) To avoid rapid degradation/aggregation, Aβ42 peptides were diluted by 10 folds with desired native nESI-MS buffer, and aliquot and flash freeze using dry ice before storage at -80 ℃ fridge.
5) To reproducibly obtain stable native nESI-MS signal, avoid repeated thawing and freezing of aliquots and it is recommended that the spray experiments should be performed as soon as the aliquots are thawed. Typical Aβ42 for nESI-MS is 2 μM in 10 mM ammonium acetate (pH 6.8), unless stated otherwise.

TWIMS CCS calibration and calculation. CCS values were calibrated using peak centroids in arrival time distributions as extracted by using MassLynx software and Driftscope map. CCS calibration curves were generated using a previously described protocol, and using literature CCS values derived for use with the Synapt instrument platform [1, 2]. CCS values for Aβ stereoisomers were calibrated with $_{D,L}$-polyalanine (3-26 alanines, 1+ and 2+) ions under the same instrument operating conditions. Nitrogen CCS values were used to construct the calibration function. Similar to our previous studies [1, 3], triplicate measurements were taken in order to obtain uncertainty values using the following equation:

$$total\_uncertainty = \sqrt{\sigma^2 + cal\_error^2 + database\_error^2}$$

where σ is the relative standard deviation of triplicate measurements (was 0.69%), *cal_error* is the uncertainty range for CCS calibration (was 0.18%), and *database_error* is the uncertainty in database values (set as 0.3%). The total uncertainty for TWIMS CCS of Aβ is thus estimated to be ~0.78%.

MTT-based Cell Viability Experiments. MTT experiments were carried out following similar protocols with previous report [4]. The human neuroblastoma Neuro-2a (N2a) cell line was purchased from the American Type Culture Collection (ATCC, Manassas, VA, USA). The cell line was maintained in media containing 1:1 Minimum Essential Media (MEM, GIBCO, Grand Island, NY, USA) and Ham's F12K Kaighn's Modification Media (F12K, GIBCO), 10% (v/v) fetal bovine serum (FBS, Sigma-Aldrich), and 1% (v/v) penicillin (GIBCO). The cells were grown and maintained at 37 ℃ in a humidified atmosphere with 5% CO_2. Aβ samples were preincubated at 37 ℃ for 24 hours to induce aggregation, and then the cell viability upon treatment of Aβ was determined by the MTT assay.

N2a cells were seeded in a 96 well plate (15,000 cells in 100 μL per well) and treated with pre-incubated (24 h) Aβ. After 24 h incubation at 37 ℃, 100 μL MTT (0.5 mg/mL in phosphate buffered saline and DMEM media) was added to each well and the plates were incubated for 2 h at 37 ℃. Remove the MTT solution by multichannel pipette, then add 100 μL DMSO to the culture well. Gently mix in a gyratory shaker or by pipetting up and down. The absorbance at 570 nm and 690 nm were measured on a microplate reader. Measure the optical density (OD) of each well by subtract absorbance at 690 nm from absorbance at 570 nm. Measure the relative viability (RV) by following formula:

$$RV = \frac{OD\ of\ sample - OD\ of\ blank\ control}{OD\ of\ negative\ control - OD\ of\ blank\ control} * 100\%$$

OpenSPR. We select OpenSPR as a tool for the discrimination of chiral Aβ binding behavior, as OpenSPR™ is a powerful instrument providing in-depth label-free binding kinetics for a variety of different molecular interactions. One of the most common applications of surface plasmon resonance is the analysis and quantification of the interactions between proteins. SPR experiments were performed using a Nicoya Lifesciences OpenSPR system equipped with a COOH chip. Following the start-up procedure found in the OpenSPR™ manual, setup the OpenSPR™ instrument and load a COOH Sensor Chip. The COOH surface was activated following the instructions included in the Amine kit. The ligand was diluted to a concentration of 45 μg/mL into immobilization buffer (provided by Nicoya Lifesciences, pH 4.5) and 100 μL was injected at 20 μL/min for a 5-minute interaction time. Aβ antibody (6E10) was immobilized using standard procedures. Immobilization was monitored via absorbance change in a standard solution of filtered buffer (PBS, pH 6.8, with 0.005% Tween 20) for 5 minutes at a flow rate of 50 μl/min. The surface was blocked with an injection of 100 μL of blocking buffer (provided by Nicoya Lifesciences, 1 M ethanolamine, pH 8.5). The flow rate was increased to 50 μL/min, and the analyte was injected at the concentrations as indicated in related figures. An association time of 150 seconds and a dislocation time of 400 seconds were used. The surface was regenerated with an injection of regeneration buffer (HCl 10 mM, pH 2.0) at a speed of 150 μL/min between each analyte injection. The chip was washed in 10 mM HCl (pH 2.0) to remove impurities. Data were collected at a rate of 5 Hz and was single referenced with blank injections. Data were fit to a 1:1 interaction model using the analysis software TraceDrawer.

Native IM-MS. Each sample of approximately 5 μL was loaded into a home-made nanospray ion source, and a 100 μm thick silver wire of was inserted into the borosilicate glass needle for high voltage application. All peptide samples were prepared in 10 mM NH_4OAc (if not otherwise specified). All reactions were monitored after incubation in a water bath at 37 ℃ for at least three hours. Approximately 5 μL of each sample was loaded into the nanospray source and the MS instrument was run in positive ion mode. Nanospray voltages ranged between 1.0-2.0 kV and the sampling cone was used at 30 V. In typical nanospray experiments, the size of the spray emitter was maintained at ~5 μm. The emitters were pulled from borosilicate glass capillaries using a P-2000 laser-based micropipette puller (Sutter Instruments, Novato, CA, USA). All IM-MS data were collected using Waters Synapt G2 instrument (Waters, Milford, MA, USA). The MS cone temperature was 75 ℃. The Synapt instrument was tuned to allow preservation and transmission of native proteins and protein interactions. This typically involved elevated pressures in the source region (~6 mbar), and decreasing all focusing voltages (e.g., cone, extractor, and bias voltages). The traveling-wave ion mobility separator was operated at a pressure of ~3.5 mbar, and DC voltage waves (30 V wave height traveling at 400 m/s) to generate ion mobility separation. CIU was achieved by increasing the trap CE from 10-170V with a step voltage of 10 V.

IM-MS-guided REMD simulation. Molecular dynamics (MD) simulations were performed with CHARMM on a workstation with 48 CPU core 2.10 GHz Intel Xeon Processor. The CHARMM36 force field [5] was employed for all MD simulations. The input models were generated on CHARMM with experimentally observed peptide sequences. Charges were placed on titratable residues (Lys, Arg, Glu, Asp) by protonating or deprotonating so that the net charge of the peptides corresponds to the experimentally observed charge state of peptides. These charge-placed peptides were subjected to energy minimization via steepest descent (SD) over 1000 steps. The energy minimized peptide model was used as the input for subsequent equilibration MD simulation. The equilibration was performed at 300 K over 200 ps timescale with simulation time step of 2 fs. The final equilibrated structure was then used as a starting structure for REMD simulations [6]. The REMD runs utilized 12 replicas ranging from 300 K to 600 K over 150 ns simulation timescale. The exchange frequency was set to 1 ps. Structures from REMD were extracted from all REMD trajectory files. These structures were filtered based on the experimental CCSs.

The theoretical CCS values of all models were calculated using IMPACT [7] due to the large number of models generated from MD simulations. To increase the accuracy of CCS calculations, 2000 structures were randomly selected from the extracted structures, and Collidoscope [7] was used for trajectory method (TM) CCS calculations. The IMPACT projected area (PA) CCS and Collidoscope TM CCS were plotted,

and a regression was used to build a calibration function to correct the rapid IMPACT PA CCS values into approximated TM CCS values for all the structures. All extracted structures were filtered based on the experimental CCSs. The filtered models were then clustered for their structural similarities based on Kabsch's RMSD analysis [8].

Trapped ion mobility spectrometry (TIMS)-MS experiments. Trapped ion mobility spectrometry (TIMS) measurements were performed on timsTOF Pro (Bruker Corp.) operated in MS1 mode, with TIMS on, over the *m/z* range 100-1700, ramp time 100 ms. Low-concentration electrospray ionization (ESI) tune mix (Agilent Technologies, Santa Clara, CA, P/N G1969-85010) calibration solution was directly infused using a standard ESI source (Bruker Corp.) for both quadratic TOF calibration and linear calibration of the TIMS analyzer over a 1/k0 window of (0.6, 1.6) $V \cdot s \cdot cm^{-2}$. After charge states were assigned to dominant masses in the mobilogram using dataAnalysis 5.2 (Bruker Corp.), the experimental peptide CCSs were deduced based on tuning mix ions 622.0, 922.0 and 1222.0 as external calibrants.

Improved md-IM-MS Separation of Aβ42 N Terminus and Core Region Fragments. We adapt our previously reported metal-enhanced chiral separation strategy [9, 10] for resolving these more complex stereoisomers on both TWIMS and a trapped IMS (TIMS) platform. Two key elements for md-IM-MS consist of metal coordination and three-dimensional (3D) CCS scattering (**Figures S6/7**) in a 3D space (x, y, z) of apo-, 1-copper-bound and 2-copper-bound ion species for 1D (x coordinate), 2D (y coordinate) and 3D (z coordinate), respectively. On top of these 3D scattering maps, a quantitative parameter, Structural Difference between D and L stereoisomers (DLSD, **Figures S8**), is calculated based on the spatial distance in the 3D space and used to characterize the improved CCS resolving capability.

Although in our previous report we tested the singly charged fragments as a proof of concept demonstration [9], examining the dominant doubly charged fragments allows more accurate information on the solution structures. Likely, the chiral amplification strategy works well for doubly charged Aβ42 core region fragments (**Figure S8**). It should be noted that, some noticeable differences of CCS values between TWIMS and TIMS measurements were observed as well as their spatial distribution in the 3D scattering maps (upper and middle panel in **Figure S6**). To minimize this type of instrument-dependent variations, we propose a new experimental group, "Composite" group, which averages the TWIMS and TIMS results (i.e. triplicate CCS values). Accordingly, the DLSDs for Composite group (**Figure S8**) are calculated from corresponding composite CCS values (lower panel in **Figure S7**). For all stereoisomers of Aβ core region fragments, an increasing trend of DLSD values was observed across 1D, 2D and 3D separation. These results suggest the improved chiral amplification performance with multi-IM device-equipped md-IM-MS strategy.

However, in addition to DLSD values, the CCS changing trend would be more relevant for the molecular dissection of Aβ stereochemistry. As such, CCS changing ratios for different Aβ stereoisomers were calculated across TWIMS, TIMS and Composite group. While TWIMS cannot resolve Aβ N terminus stereoisomers, the TIMS and Composite group show moderate separation results and all N terminus stereoisomers hold increased CCS values by ~1.3% (**Figure S9**). Conversely, the composite CCS values for Aβ core region stereoisomers are decreased by ~1.1%. Given the total CCS uncertainty range is around 0.78% in our experiments, the observed trend in CCS is indicative of meaningful structural alteration.

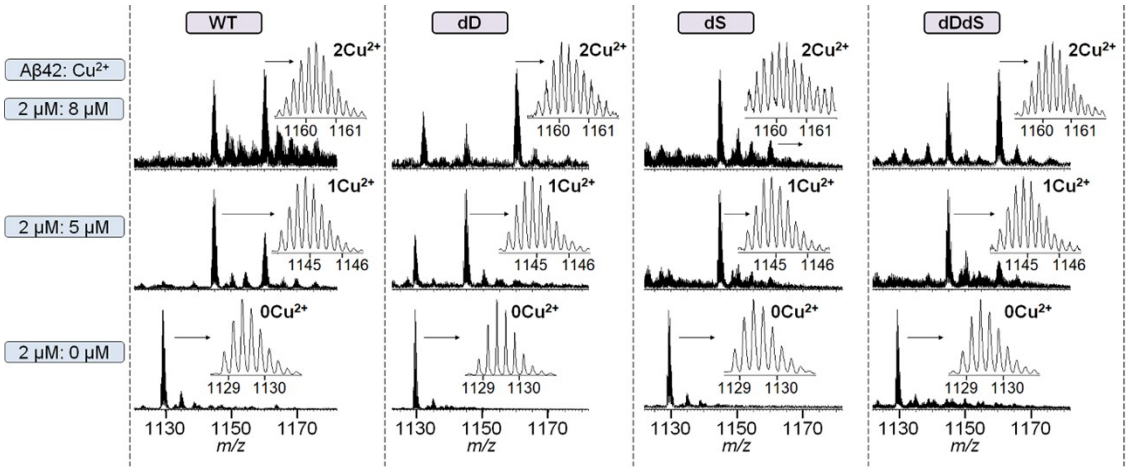

Figure S1. Representative MS spectrum for Aβ42-Cu^{2+} binding system. Notably, $0Cu^{2+}$, $1Cu^{2+}$, and $2Cu^{2+}$ labels indicate different binding states for Aβ42 stereoisomers, zero copper, one copper and two copper-bound, respectively.

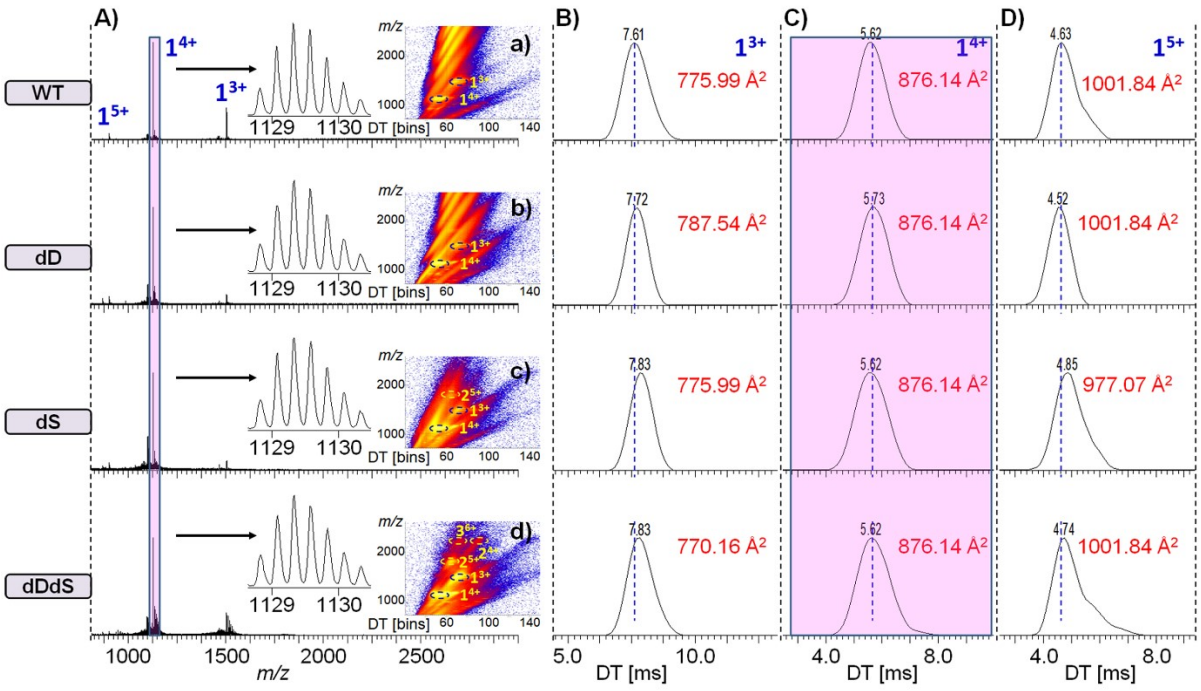

Figure S2. Chiral differentiation of full-length Aβ42 stereoisomers (WT/dD/dS/dDdS) by using TWIMS instrument. (A) Representative mass spectra for four Aβ42 stereoisomers with isotopic distributions of 4+ inserted. Individual IM heatmaps (a-d) are also shown. (B-D) TWIMS drift time distributions for Aβ42 stereoisomeric monomer 3+ to 5+, respectively. Aβ42, 2 μM. Buffer, 10 mM ammonium acetate.

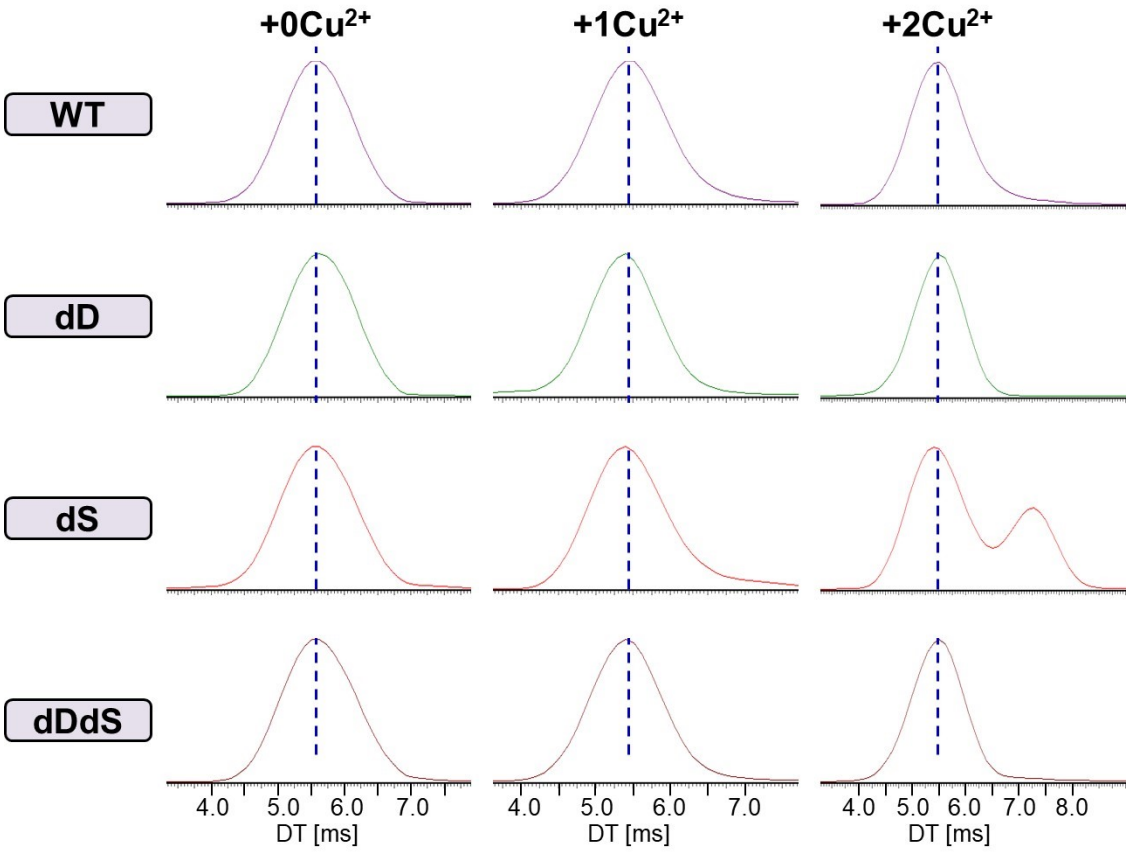

Figure S3. Representative TWIMS-measured drift time (DT) distributions for Aβ42 stereoisomers (4+, WT/dD/dS/dDdS) with different levels of copper complexation. Aβ42, 2 μM. Cu^{2+}, 8 μM. Buffer, 10 mM NH_4OAc.

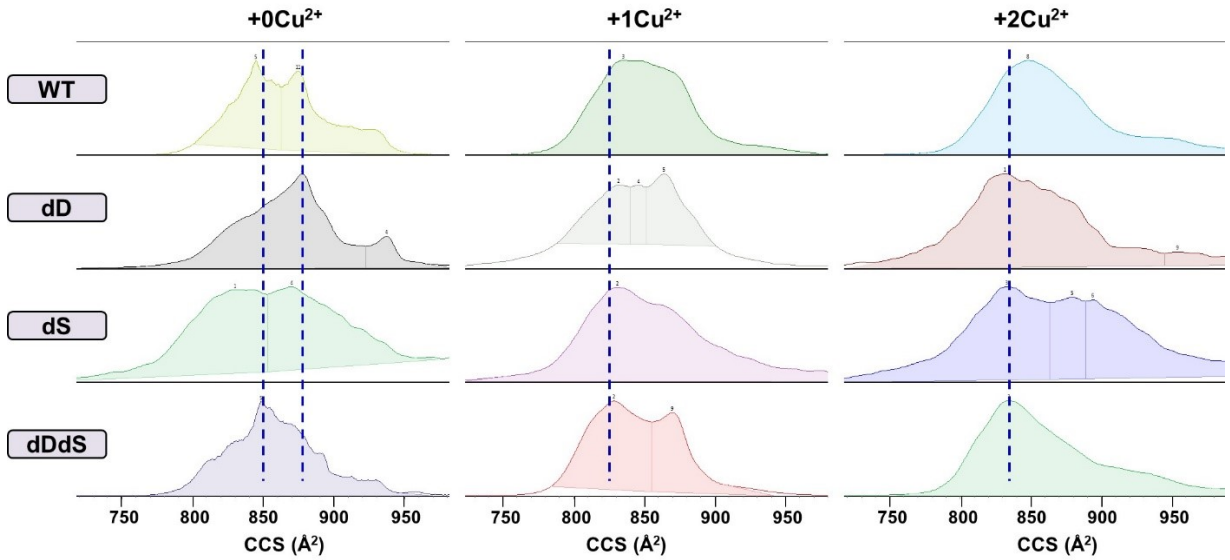

Figure S4. Representative TIMS-measured CCS distributions for Aβ42 stereoisomers (4+, WT/dD/dS/dDdS) with different levels of copper complexation. Aβ42, 2 μM. Cu^{2+}, 8 μM. Buffer, 10 mM NH_4OAc.

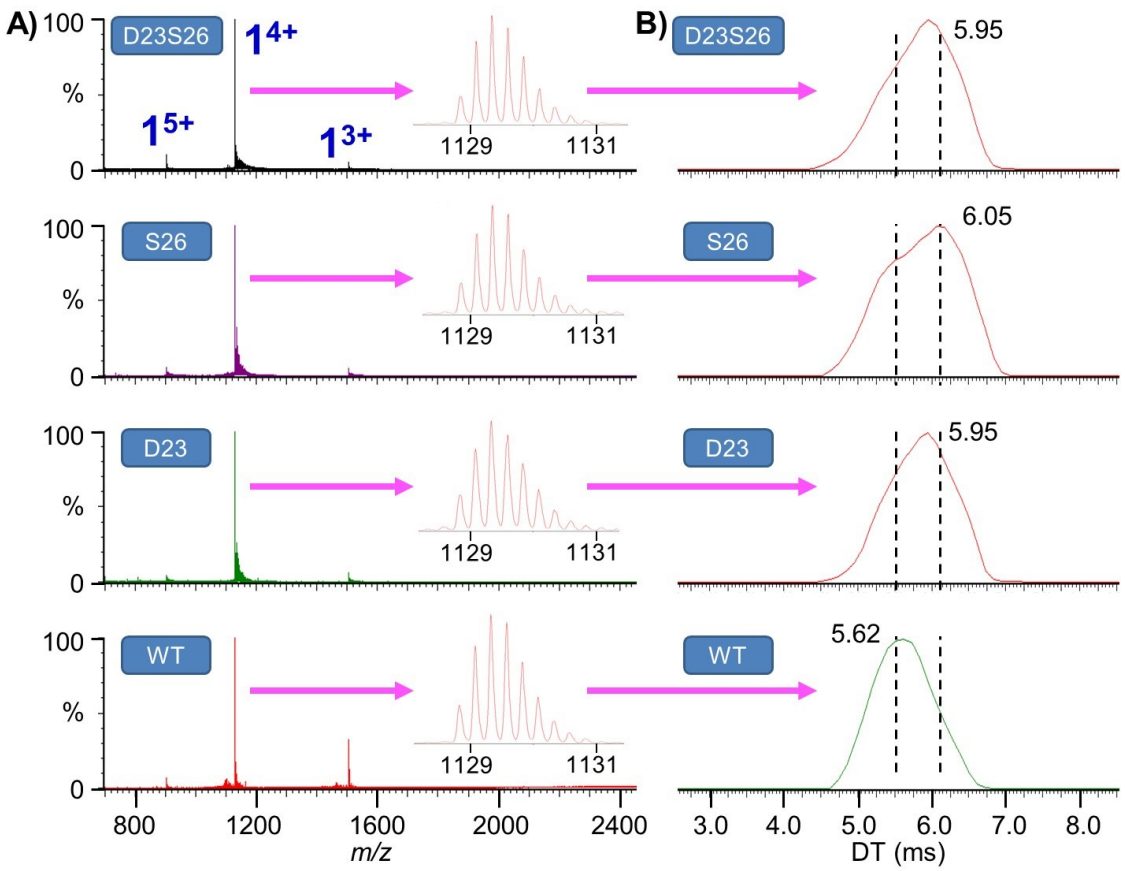

Figure S5. Chiral differentiation of full-length Aβ42 stereoisomers (WT/D23/S26/D23S26) by using the TWIMS instrument. (A) Representative mass spectra for four Aβ42 stereoisomers with isotopic distributions of 4+ inserted. (B) TWIMS drift time distributions for Aβ42 stereoisomeric monomer 4+. Aβ42, 2 μM. Buffer, 10 mM ammonium acetate.

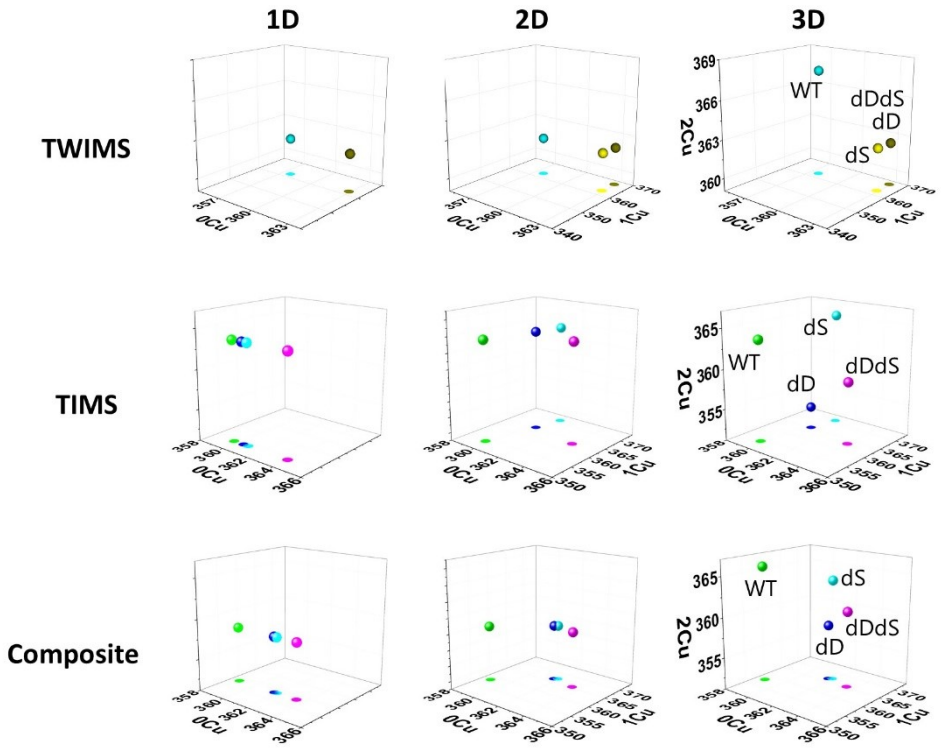

Figure S6. Individual scattering maps for 1D, 2D and 3D discrimination of Aβ42 N-terminus fragments (WT/dD/dS/dDdS Aβ10) based on average CCS values of 2+ ion species from triplicate measurements (average RSDs < 0.5%, errors not shown). The "Composite" group generally averages TWIMS and TIMS measurements, which is designed to unbiasedly amplify chiral differences. Note, similar data integration results have been reported in a recent paper by our group (*Anal. Chem.* 2023, 95, 2221-2228).

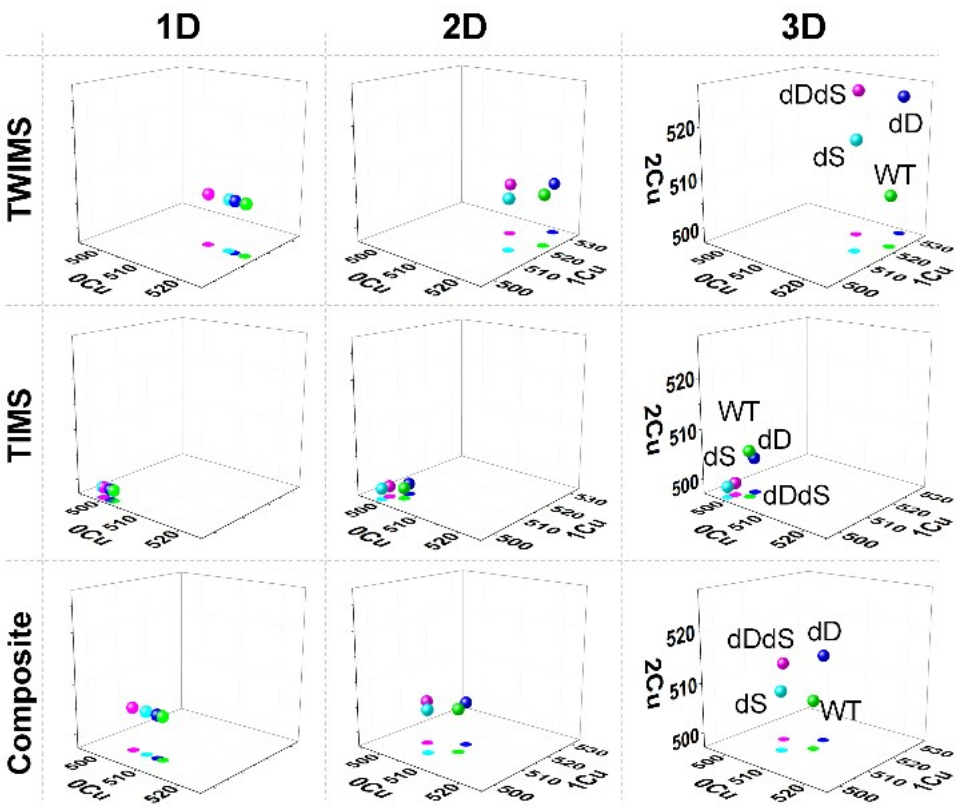

Figure S7. Individual scattering maps for 1D, 2D and 3D discrimination of Aβ42 core region fragments (WT/dD/dS/dDdS Aβ17-36) based on average CCS values of 2+ ion species from triplicate measurements (average RSDs < 0.5%, errors not shown). The "Composite" group generally averages TWIMS and TIMS measurements, which is designed to unbiasedly amplify chiral differences.

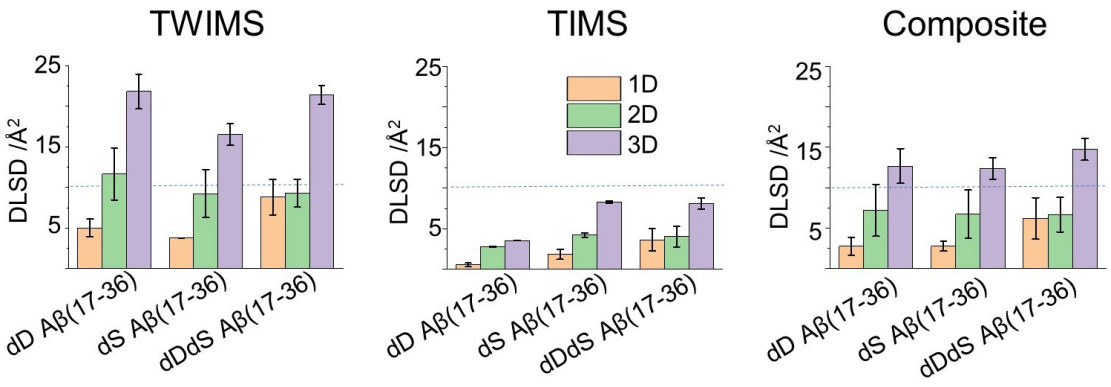

Figure S8. Structural differences between D and L stereoisomers (DLSD) as calculated from 1D/2D/3D scattering plots (Figure S7) for core region fragments. Error bars, S.D. from triplicate measurements.

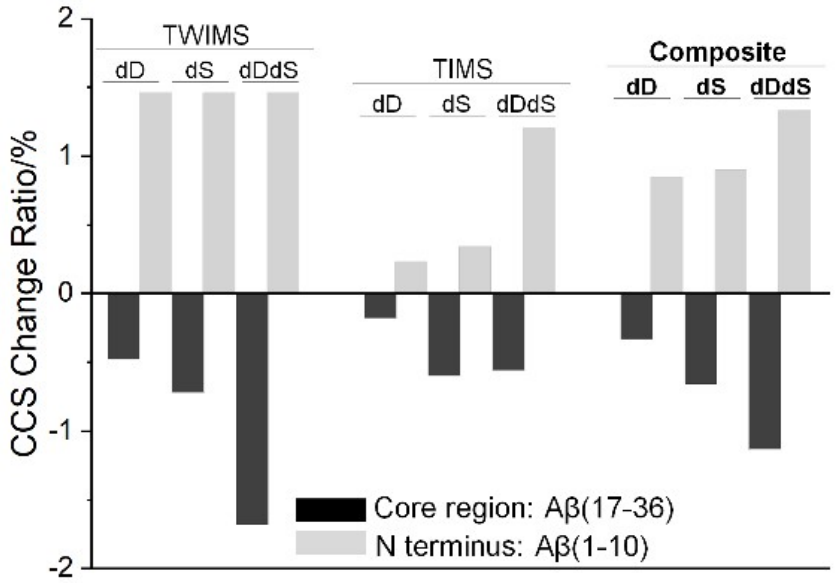

Figure S9. CCS changing trends for stereoisomers of Aβ42 N terminus and core region fragments as calculated from the average CCS values (data in Figures S6/7). Average CCS values (data in Figures S6/7) are calculated based on doubly charged ion species, which is different from our previous report where singly charged ion CCSs were used [9].

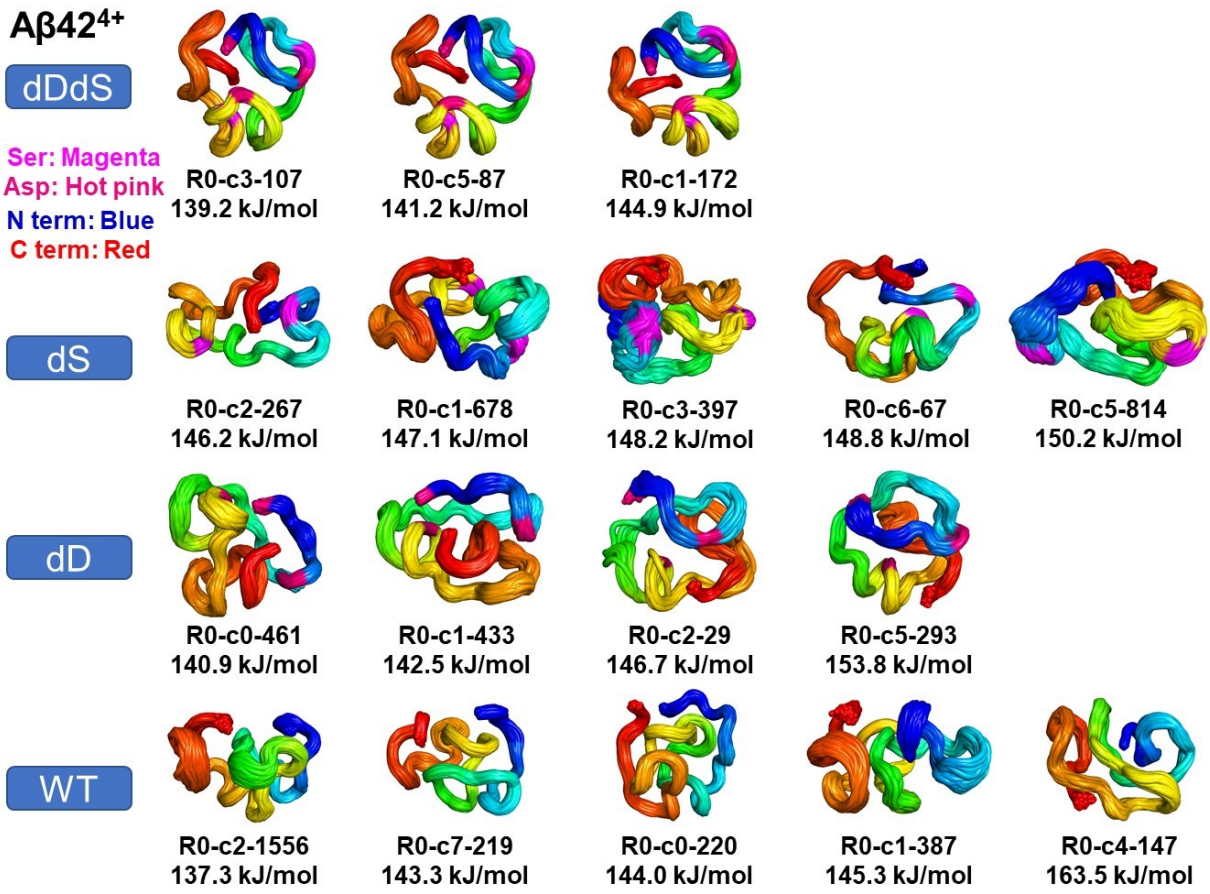

Figure S10. Energetically favorable REMD structures for Aβ42 stereoisomers of 4+ ion species. All structures are filtered by TIMS-CCS(N_2) with 3% calibration error; conformations at 300 K (lowest temperature) were clustered and listed are the most confidently identified REMD clusters (population > 1% with well-aligned structures). R0-c3-107: R0 (rep #0), c3 (cluster #3), 107 (total pdb model numbers). N-terminus, blue; C-terminus, red; Ser residues, magenta; Asp residues, hot pink. Energy for each conformer is also listed right below the cartoon illustration.

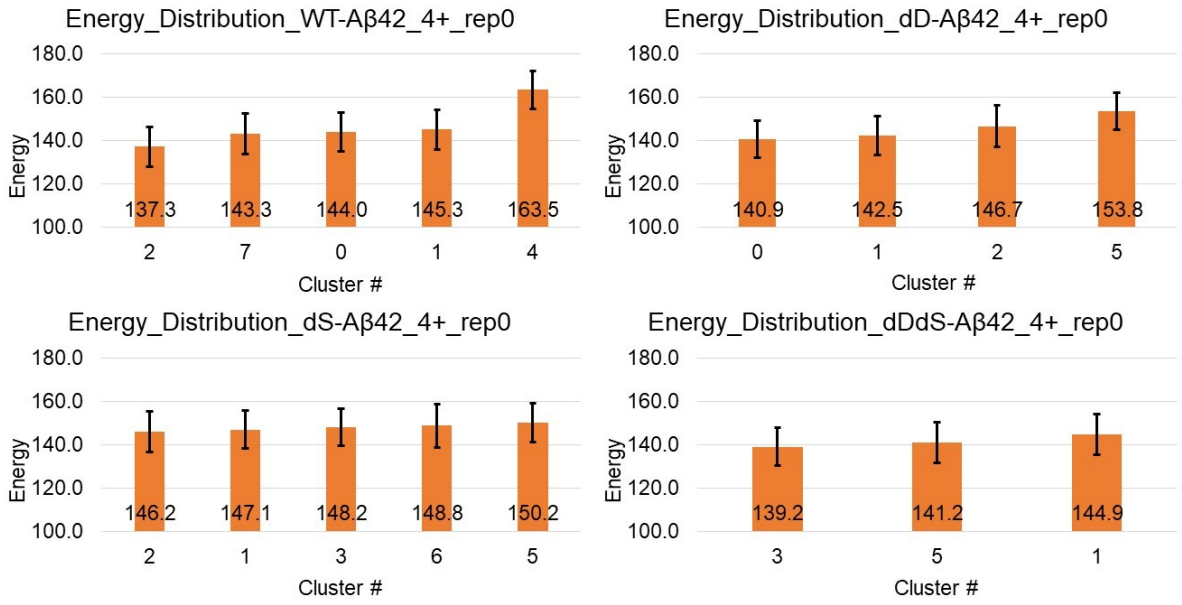

Figure S11. Energy distributions for REMD structural models of Aβ42 stereoisomers of 4+ ion species.

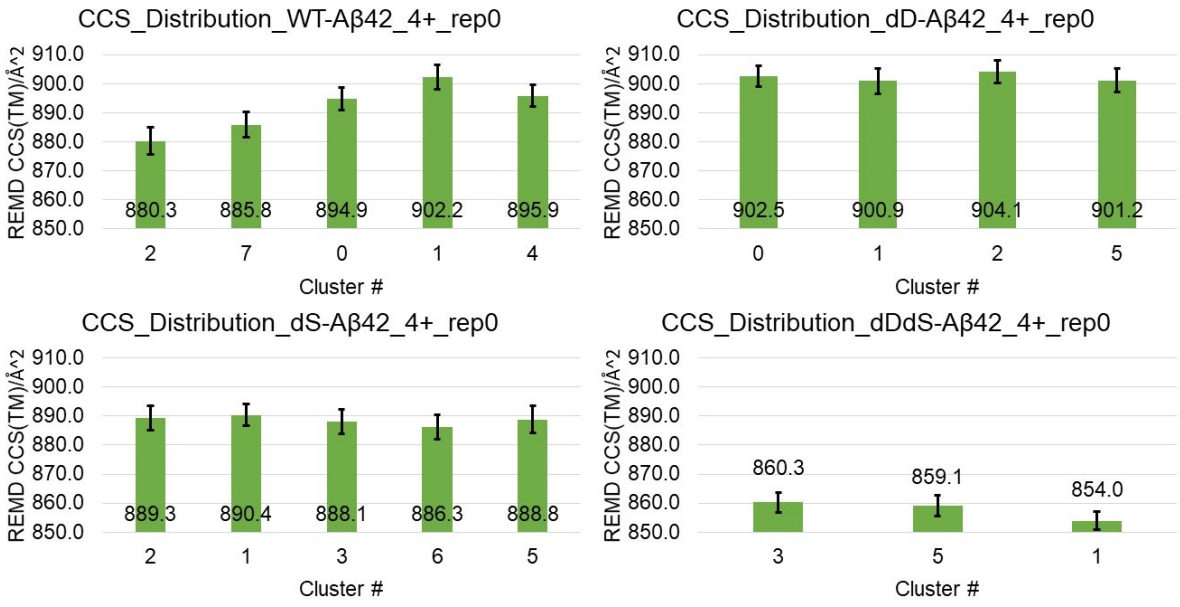

Figure S12. CCS distributions for REMD structural models of Aβ42 stereoisomers of 4+ ion species.

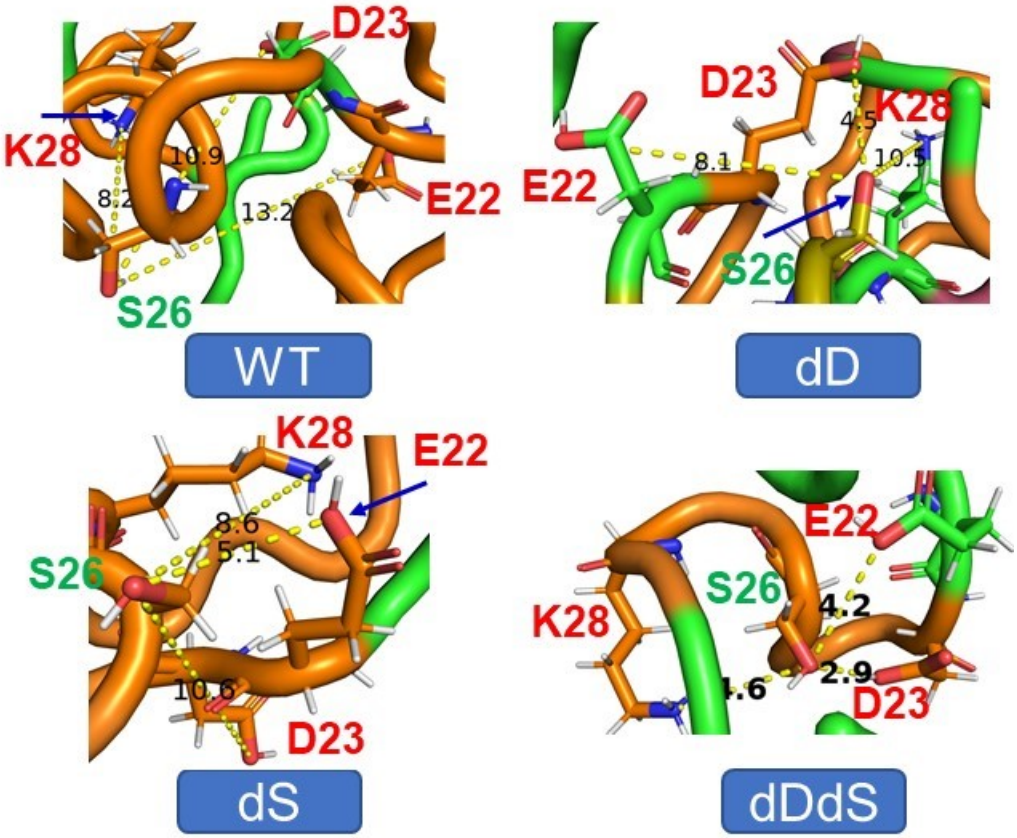

Figure S13. REMD lowest energy cluster and charge-dipole interactions of Aβ42 stereoisomers of 4+ ion species centering around Ser26 residue.

Supplementary References

1. B. T. Ruotolo, J. L. Benesch, A. M. Sandercock, S. J. Hyung and C. V. Robinson, Ion mobility-mass spectrometry analysis of large protein complexes, *Nat. Protoc.*, 2008, **3**, 1139-1152.
2. M. F. Bush, Z. Hall, K. Giles, J. Hoyes, C. V. Robinson and B. T. Ruotolo, Collision Cross Sections of Proteins and Their Complexes: A Calibration Framework and Database for Gas-Phase Structural Biology, *Anal. Chem.*, 2010, **82**, 9557-9565.
3. D. A. Polasky, S. M. Dixit, M. F. Keating, V. V. Gadkari, P. C. Andrews and B. T. Ruotolo, Pervasive Charge Solvation Permeates Native-like Protein Ions and Dramatically Influences Top-down Sequencing Data, *J. Am. Chem. Soc.*, 2020, **142**, 6750-6760.
4. T. S. Choi, H. J. Lee, J. Y. Han, M. H. Lim and H. I. Kim, Molecular Insights into Human Serum Albumin as a Receptor of Amyloid-beta in the Extracellular Region, *J. Am. Chem. Soc.*, 2017, **139**, 15437-15445.
5. B. R. Brooks, C. L. Brooks, 3rd, A. D. Mackerell, Jr., L. Nilsson, R. J. Petrella, B. Roux, Y. Won, G. Archontis, C. Bartels, S. Boresch, A. Caflisch, L. Caves, Q. Cui, A. R. Dinner, M. Feig, S. Fischer, J. Gao, M. Hodoscek, W. Im, K. Kuczera, T. Lazaridis, J. Ma, V. Ovchinnikov, E. Paci, R. W. Pastor, C. B. Post, J. Z. Pu, M. Schaefer, B. Tidor, R. M. Venable, H. L. Woodcock, X. Wu, W. Yang, D. M. York and M. Karplus, CHARMM: the biomolecular simulation program, *J. Comput. Chem.*, 2009, **30**, 1545-1614.
6. Y. Sugita and Y. Okamoto, Replica-exchange molecular dynamics method for protein folding, *Chem. Phys. Lett.*, 1999, **314**, 141-151.
7. Erik G. Marklund, Matteo T. Degiacomi, Carol V. Robinson, Andrew J. Baldwin and Justin L. P. Benesch, Collision Cross Sections for Structural Proteomics, *Structure*, 2015, **23**, 791-799.
8. W. Kabsch, A solution for the best rotation to relate two sets of vectors, *Acta Crystallogr. A*, 1976, **32**, 922-923.
9. G. Li, K. DeLaney and L. Li, Molecular basis for chirality-regulated Abeta self-assembly and receptor recognition revealed by ion mobility-mass spectrometry, *Nat. Commun.*, 2019, **10**, 5038.
10. X. Xu, L. Han, Z. Zheng, R. Zhao, L. Li, X. Shao and G. Li, Composite Multidimensional Ion Mobility-Mass Spectrometry for Improved Differentiation of Stereochemical Modifications, *Anal. Chem.,* 2023, **95**, 2221-2228.